A LETTERS JOURNAL EXPLORING THE FRONTIERS OF PHYSICS

LETTER

Self-organised criticality in stochastic sandpiles: Connection to directed percolation

To cite this article: Urna Basu and P. K. Mohanty 2014 *EPL* **108** 60002

A Letters Journal Exploring the Frontiers of Physics
December 2014
EPL, **108** (2014) 60002 www.epljournal.org
doi: 10.1209/0295-5075/108/60002

Self-organised criticality in stochastic sandpiles: Connection to directed percolation

Urna Basu[1] and P. K. Mohanty[2,3]

[1] *Instituut voor Theoretische Fysica, KU Leuven - 3000 Leuven, Belgium*
[2] *CMP Division, Saha Institute of Nuclear Physics - 1/AF Bidhan Nagar, Kolkata-700064, India*
[3] *Max-Planck-Institut für Physik komplexer Systeme - Nöthnitzer Strasse 38, 01187 Dresden, Germany*

received 11 October 2014; accepted in final form 1 December 2014
published online 23 December 2014

PACS 05.65.+b – Self-organized systems
PACS 68.35.Rh – Phase transitions and critical phenomena
PACS 64.60.ae – Renormalization-group theory

Abstract – We introduce a stochastic sandpile model where finite drive and dissipation are coupled to the activity field. The absorbing phase transition here, as expected, belongs to the directed percolation (DP) universality class. We focus on the small drive and dissipation limit, *i.e.* the so-called self-organised critical (SOC) regime and show that the system exhibits a crossover from ordinary DP scaling to a dissipation-controlled scaling which is independent of the underlying dynamics or spatial dimension. The new scaling regime continues all the way to the zero bulk drive limit suggesting that the corresponding SOC behaviour is only DP, modified by the dissipation-controlled scaling. We demonstrate this for the continuous and discrete Manna model driven by noise and bulk dissipation.

Introduction. – Sandpile models [1–10] show scale free avalanche patterns and are taken as prototype models of self-organized criticality (SOC). In these models sand grains (particles or energy) are added randomly to an empty lattice. Whenever the number of grains in a site crosses a predefined threshold value, it becomes unstable (active) and relaxes by toppling. In a toppling event, particles or energy from each active site is redistributed among the neighbours, which may further create new topplings. Such a cascade of toppling events, commonly known as an avalanche, continues in the system until all sites become stable (inactive); a new grain is added then. The large avalanches usually hit the boundary where some energy is dissipated out of the system. The interplay of the slow driving, fast relaxation, and dissipation at the boundaries brings in a self-organized critical state without any fine-tuning of parameters. It is well known that the critical behaviour of sandpile models with stochastic toppling rules differ from that of those having deterministic dynamics and form a generic universality class, namely the Manna class [6].

It was argued by Dickman and co-workers [11], and supported by several other works [12], that the critical behaviour of SOC can be understood as an ordinary absorbing phase transition (APT) in a fixed energy sandpile (FES). The slow drive and boundary dissipation in SOC ensure that density gets adjusted to the critical value. Since the most robust universality class of absorbing state phase transitions is DP, one naturally asks whether the self-organised criticality of stochastic sandpile models is in any way connected to DP. This doubt is bolstered by the fact that the exponents of the Manna class are not very different from DP. Several attempts have been made over the last decades to understand this riddle [13–15]. In fact, both stochastic and deterministic sandpile models flow to DP when perturbed [14]. It was also suggested recently that the ordinary critical behaviour of fixed energy stochastic sandpiles belongs to DP [16], though this issue is still being debated [17]. All these works raise a possibility that the observed self-organised criticality in stochastic sandpile models is also related to DP.

In this letter we attempt to explore this possibility and bridge the gap between DP and SOC. Conventionally self-organised sandpile models are studied with dissipation only at the boundaries. Another equivalent approach, where dissipation is incorporated in the bulk of a closed system [14,18], has certain advantages; it avoids difficulties like non-zero particle current from the bulk towards the boundary [19,20], inhomogeneous correlated height profiles [13] and other unusual boundary effects [15]. Here we

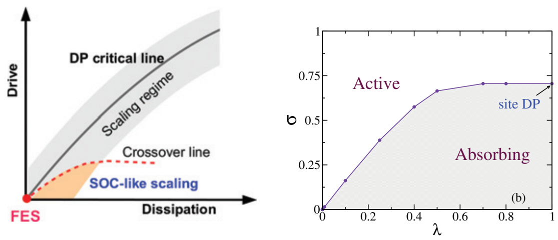

Fig. 1: (Colour on-line) (a) Schematic phase diagram: the grey shaded area represents the scaling regime around the DP critical line. In the small drive-dissipation regime, the crossover line (dashed) separates ordinary DP and SOC-like scaling (orange shaded area). Ordinary DP scaling disappears in the zero drive limit. (b) The actual phase diagram for the driven dissipative Manna model in $1d$.

choose to work with bulk dissipation (parametrized by λ) and introduce the additional finite drive σ coupled to the activity in a way that the dynamics of the driven dissipative sandpile model reduces to SOC in the $\sigma \to 0$ limit and site DP when $\lambda \to 1$. We find that in the small drive-dissipation limit, a new scaling regime emerges in the subcritical phase when one moves away from the critical λ_c —observables which ordinarily scale as $(\lambda - \lambda_c)^a$ crosses over to $(\lambda - \lambda_c)^{\tilde{a}}$. We argue that the new exponent $\tilde{a}$ can be expressed in terms of the known DP exponents a and γ as

$$\tilde{a} = a/\gamma. \tag{1}$$

This new scaling regime persists all the way down to the $\sigma = 0$ line suggesting, first, that what is commonly know as bulk dissipative SOC (for $\sigma = 0$ and small λ) is nothing but DP with modified scaling, and secondly, that a SOC-like behaviour can also be observed in systems with finite drive and dissipation, both local. A schematic representation of this scenario is presented in fig. 1(a). We use a numerical simulation to verify this picture for the continuous Manna model in one dimension ($1d$) and $2d$, and the discrete Manna model in $1d$.

Driven dissipative continuous Manna model. – The driven dissipative continuous Manna model can be defined on a general graph as follows. Each site $\mathbf{R}$ on the graph has a continuous variable $E_{\mathbf{R}}$, called energy, associated with it; sites with $E_{\mathbf{R}} \geq 1$ are declared active. At any given instant, let S_a be the set of active sites and S_n, the set of neighbours of the active sites (which may or may not be active). The dynamics proceeds as a three-step parallel update:
I. *Dissipation*: All sites belonging to $\mathcal{S}_a \cup \mathcal{S}_n$, *i.e.* the sites which are active themselves or have at least one active neighbour, dissipate the λ fraction of their energies,

$$E_{\mathbf{R}} \to (1-\lambda)E_{\mathbf{R}} \quad \forall\, \mathbf{R} \in \mathcal{S}_a \cup \mathcal{S}_n. \tag{2}$$

II. *Distribution*: All active sites distribute their remaining energy randomly among the neighbours, *i.e.* for all $\mathbf{R} \in \mathcal{S}_a$, if $N_{\mathbf{R}}$ is the set containing neighbours of $\mathbf{R}$

$$\begin{aligned} E_{\mathbf{R}'} &\to E_{\mathbf{R}'} + r_{\mathbf{R}'} E_{\mathbf{R}} \quad \forall\, \mathbf{R}' \in N_{\mathbf{R}} \\ \text{and } E_{\mathbf{R}} &\to 0 \quad \forall\, \mathbf{R} \in \mathcal{S}_a, \end{aligned} \tag{3}$$

where $\{r_{\mathbf{R}'} \in (0,1)\}$ are random numbers satisfying

$$\sum_{\mathbf{R}' \in N_{\mathbf{R}}} r_{\mathbf{R}'} = 1.$$

III. *Drive*: Finally, the drive is added with probability σ independently to all the sites belonging to $\mathcal{S}_n$ (*i.e.* the receiving sites) in the form of

$$E_{\mathbf{R}} \to E_{\mathbf{R}} + 1 \quad \text{with probability } \sigma. \tag{4}$$

Note that, in this dynamics, the energy is added to or dissipated from the system only when it is active, ensuring that absorbing configurations are not spontaneously activated by noise.

Some of the limiting cases of this dynamics are of special interest. Without any drive or dissipation $\sigma = 0 = \lambda$, this model maps to the conserved continuous Manna model (CCMM) in d-dimension [16]; the conserved density needs to be tuned to locate the absorbing phase transition in this fixed energy sandpile model. On the other hand, when $\lambda = 1$, the active site surely becomes inactive after each update, and each of the sites which have at least one active neighbour gets activated itself with probability σ. This is the dynamics of site-directed percolation; thus for $\lambda = 1$ the present model would show an absorbing state transition at [21]

$$\sigma_c^{DP} = \begin{cases} 0.705489, & d = 1, \\ 0.34457, & d = 2, \text{ square lattice.} \end{cases} \tag{5}$$

For non-zero noise and dissipation, the parameters λ and σ control the average energy of the system. However, the absorbing configurations of this model are no different from those of CCMM since the additional dynamics I. and III. cannot be executed on inactive states. For any given λ, the system is expected to fall into an absorbing configuration when σ is decreased below a critical threshold $\sigma_c(\lambda)$. Since the model satisfies all the criteria of the DP conjecture [22], one naturally expects that the critical behaviour along the critical line $\sigma_c(\lambda)$, which includes the site DP critical point ($\lambda = 1, \sigma = \sigma_c^{DP}$), would belong to the DP universality class.

Let us consider the $d = 1$ case in detail. On a one-dimensional periodic lattice with L sites $i = 1, 2, \ldots, L$, each having a continuous variable called energy E_i, the three-step parallel dynamics reads as follows. (I.) All sites belonging to $\mathcal{S}_a \cup \mathcal{S}_n$, dissipate the λ fraction of their energies $E_i \to (1-\lambda)E_i$. (II.) Then the active sites distribute their remaining energy randomly among the two neighbours, *i.e.* $E_{i\pm1} \to E_{i\pm1} + [\frac{1}{2} \pm (r_i - \frac{1}{2})]E_i$ and $E_i \to 0$. Here r_i is a random number distributed uniformly in $(0,1)$. (III.) Finally, all the sites $i \in \mathcal{S}_n$, are activated by adding unit energy independently and randomly with probability σ, *i.e.*, $E_i \xrightarrow{\sigma} E_i + 1$.

Table 1: Directed percolation exponents along with the modified values in SOC-like scaling.

	τ_s	γ	κ_s	τ_t	τ	κ_t	$\tilde{\gamma}$	$\tilde{\kappa}_s$	$\tilde{\tau}$	$\tilde{\kappa}_t$
$1d$	1.108	2.277	2.553	1.159	1.45	1.724	1	1.121	0.636	0.757
$2d$	1.267	1.594	2.174	1.457	0.712	1.295	1	1.364	0.447	0.812

We have studied the absorbing state phase transition here for a set of values of λ taking σ as the tuning parameter σ and verified explicitly that the whole critical line $\sigma_c(\lambda)$, shown in fig. 1(b) belongs to the DP universality class. For details of this study see the supplementary text in [23].

Our main aim is to study the small drive-dissipation limit of this dynamics and to relate the critical behaviour to SOC. One way is to generate clusters from a single seed in the sub-critical regime of the APT and ask if their statistics close to the critical point relates to that of SOC [24]. To this end, starting from a fully active state, first the system is allowed to relax; absorbing configurations are then activated by generating a seed at a randomly chosen site by adding one unit of energy [25]. This *seed-simulation process* is repeated to obtain statistics of the clusters generated. For any fixed σ the clusters are expected to be characterised by DP critical exponents and scaling functions,

$$P(s) \sim s^{-\tau_s} f(s\Delta^{\kappa_s}); \qquad P(T) \sim T^{-\tau_t} g(T\Delta^{\kappa_t}), \quad (6)$$

Here $\Delta \equiv \lambda - \lambda_c$, and s, T denote the size and lifetime of clusters. Consequently their averages diverge as $\langle s\rangle \sim \Delta^{-\gamma}$ and $\langle T\rangle \sim \Delta^{-\tau}$ near the critical point with $\gamma = \kappa_s(2-\tau_s)$ and $\tau = \kappa_t(2-\tau_t)$ (see table 1). However, the average energy added and dissipated per cluster must balance to maintain a stationary state; this puts an additional constraint [26] on $\langle s\rangle$, effective primarily in the small drive regime, and prompts

$$\langle s\rangle \sim \Delta^{-1}. \quad (7)$$

This opens up the possibility that $\langle s\rangle$ might show a different scaling for a small drive σ.

Figure 2(a) shows plots of $\langle s\rangle$ as a function of $\Delta \equiv \lambda - \lambda_c$ for different values of σ including 0. For large σ the average cluster size diverges as $\langle s\rangle \sim \Delta^{-\gamma}$ with $\gamma = 2.277$ as expected for DP. However, a new scaling regime emerges as σ is decreased; $\langle s\rangle$ shows a crossover from the DP behaviour to $\langle s\rangle \sim \Delta^{-\tilde{\gamma}}$ with $\tilde{\gamma} = 1$ as λ is increased further away from the corresponding critical point $\lambda_c(\sigma)$. We must emphasize that this crossover is *not* an artefact of long relaxation time or small system size. If that were the case, unusual scaling would rather appear closer to the critical point as opposed to what we see here, *i.e.* the DP critical behaviour prevails near the critical line. This endorses the fact that the cluster statistics is obtained correctly —the system is fully relaxed and the results do not suffer from finite-size effects.

The crossover starts at smaller λ as noise strength σ is decreased; indeed for $\sigma = 0$ (lowest red curve) the DP regime completely disappears, and we only see

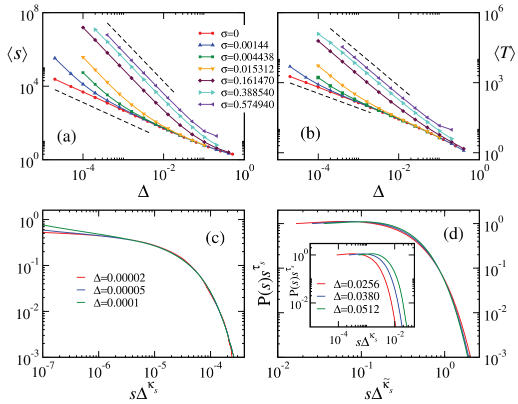

Fig. 2: (Colour on-line) (a) The average cluster size $\langle s\rangle$ and (b) average lifetime $\langle T\rangle$ *vs.* $\Delta = \lambda - \lambda_c$ for different values of σ. Panels (c) and (d) show the scaling collapse of $P(s)$ following (6): the curves corresponding to $\Delta = \lambda - \lambda_c = (2, 5, 10) \times 10^{-5}$ in (c) could be collapsed with the DP value $\kappa_s = \gamma/(2-\tau_s) = 2.55$, whereas the curves for $\Delta = 0.0256, 0.0380, 0.0512$ in (d) are collapsed with the modified exponent $\tilde{\kappa}_s = 1/(2-\tau_s) = 1.12$. Here, $L = 10^4, \sigma = 0.004438$ (corresponding critical point $\lambda_c = 0.003$) and the statistical averaging is done over 10^5 to 10^7 independent clusters.

$$\langle s\rangle \sim \lambda^{-1}. \quad (8)$$

This dissipation-controlled behaviour is characteristic to bulk dissipative SOC models [10,14]. Indeed the $\sigma = 0$ line is the SOC limit in this model as will be discussed later in this paper. Although dissipation-controlled avalanches are familiar in SOC (rather necessary to maintain a self-critical state), the possibility of their presence and effect in ordinary absorbing transitions is explored in this work. What it brings in here is a crossover from ordinary DP critical behaviour $\langle s\rangle \sim \Delta^{-\gamma}$ to Δ^{-1}. The immediate question is then whether it affects other critical exponents. Since the underlying universality is still DP (for any non-zero σ), it is natural to expect that other exponents would be modified in a way that the DP signature is retained. We put forward a conjecture that eq. (7) prompts $\Delta \to \Delta^{1/\gamma}$ and observables which ordinarily scale as Δ^a would crossover to $\Delta^{\tilde{a}}$ with $\tilde{a} = a/\gamma$. Accordingly in the new scaling regime, which we refer to as "SOC-like" regime, the cluster statistics would then be given by

$$P(s) \sim s^{-\tau_s} f(s\Delta^{\tilde{\kappa}_s}); \qquad P(T) \sim T^{-\tau_t} g(T\Delta^{\tilde{\kappa}_t}), \quad (9)$$

with $\tilde{\kappa}_{s,t} = \kappa_{s,t}/\gamma$. Consequently $\langle s\rangle = \Delta^{-\tilde{\gamma}}$ and $\langle T\rangle = \Delta^{-\tilde{\tau}}$ with $\tilde{\gamma} = \tilde{\kappa}_s(2-\tau_s) = 1$ and $\tilde{\tau} = \tilde{\kappa}_t(2-\tau_t) = \tau/\gamma$; see table 1 for the numerical values.

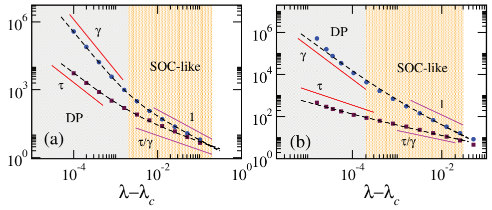

Fig. 3: (Colour on-line) The DP and SOC-like scaling regimes: (a) $1d$ driven dissipative continuous Manna model. The data used for illustration corresponds to $\sigma = 0.015312$ for which $\lambda_c = 0.01$. The dashed lines are best-fit curves obtained following eq. (10). The solid lines are for guidance. (b) The same for the $2^{10} \times 2^{10}$ square lattice, when $\sigma = 0.01$, $\lambda_c = 0.011974$. Here, statistical averaging is done over 10^4 to 10^6 clusters.

To verify this proposition we measure $\langle T\rangle$ and $P(s)$. Figure 2(b) shows $\langle T\rangle$ as a function of Δ for different values of σ. Clearly, DP behaviour prevails near the critical point, whereas the exponent that dictates $\langle T\rangle$ further away is nothing but $\tilde{\tau} = \tau/\gamma$. Change in the functional form of $P(s)$, from eq. (6) to eq. (9) can be captured from the data collapse of $P(s)s^{\tau_s}$ as a function of $s\Delta^{\kappa_s}$. As seen in fig. 2(c), the use of the DP exponent κ_s results in a perfect data collapse for small values of Δ, but fails for relatively large Δ (inset of fig. 2(d)). $P(s)$ data for larger Δ could be collapsed with modified DP exponent $\tilde{\kappa}_s = \kappa_s/\gamma$.

At this point, we arrive at the following picture —the sub-critical scaling regime of the driven dissipative Manna model in $1d$ is divided into two regions in the small drive-dissipation limit, ordinary DP scaling near the critical line crossing over to an emerging SOC-like scaling as one moves away. This is depicted in fig. 1(a) with a schematic crossover line that separates DP and SOC-like scaling; the actual phase diagram in fig. 1(b) shows the critical line.

Let us look at the generality of this scenario. Equation (8), which originates from a generic energy balance condition in the stationary state [26], is expected to hold in other stochastic sandpile models, in one and higher dimensions; the crossover from ordinary DP to SOC-like scaling in the sub-critical regime can be viewed as a generic multi-scale behaviour,

$$\langle s\rangle = A_s\Delta^{-\gamma} + B_s\Delta^{-\tilde{\gamma}}; \quad \langle T\rangle = A_t\Delta^{-\tau} + B_t\Delta^{-\tilde{\tau}}, \quad (10)$$

where the σ-dependent coefficients $A_{s,t}, B_{s,t}$ determine the crossover scale. Of course, the DP exponents γ and τ depend on the spatial dimension d, but they would still rescale as $\tilde{\gamma} = 1$, $\tilde{\tau} = \tau/\gamma$. In fig. 3(a) and (b) we verify the same for the continuous Manna model in $1d$ and $2d$, respectively. The dashed lines there are the best fit of the data points according to eq. (10), with exponents in table 1.

Now we turn our attention to the $\sigma = 0$ line. Here the unit energy added to create an active seed initiates a cluster which runs until all the sites become inactive; there is no energy input during the propagation. This is exactly how avalanches are created and propagated in the corresponding SOC models. The average energy dissipated per cluster is proportional to $\lambda\langle s\rangle$, which must balance the unit energy added initially, leading to eq. (8) under a stationary condition. This condition, as we have already mentioned, is common to *all* bulk dissipative SOC models. It also has a well-known analogue in the context of boundary dissipative sandpiles. There $\langle s\rangle \sim L^2$ [4] independently of the dynamics [27] and spatial dimension [5]. In boundary dissipative SOC models the slow dissipation required to reach a self-critical state is naturally achieved by taking $L \to \infty$. In contrast, models with bulk dissipation are studied in thermodynamically large systems and criticality is reached in the limit $\lambda \to 0$.

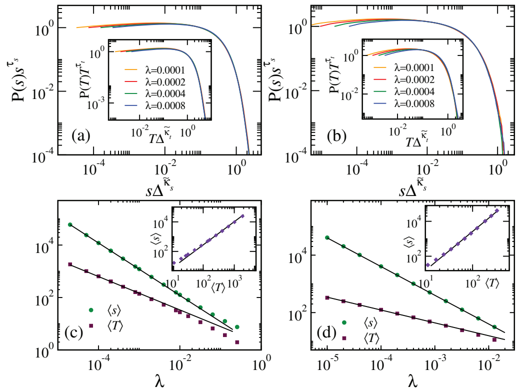

Fig. 4: (Colour on-line) The SOC limit $\sigma = 0$ for the (a) $1d$ continuous model: data collapse for $P(s)$ according to (9) with $\tilde{\kappa}_s = 1.121$ for different values of λ. The inset shows the same for $P(T)$ with $\tilde{\kappa}_t = 0.757$. (b) The same as (a) for the $2d$ continuous model. Here $\tilde{\kappa}_s = 1.364, \tilde{\kappa}_t = 0.812$. (c) Plot of $\langle s\rangle$ and $\langle T\rangle$ with λ. The corresponding exponents are $\tilde{\gamma} = 1$ and $\tilde{\tau} = .636$ (solid lines). The inset shows $\langle s\rangle \sim \langle T\rangle^{\gamma/\tau}$. Panels (b) and (d) are the same as (a) and (c), but for the $2d$ continuous model with exponents in table 1.

Next we explore whether the modified DP scaling seen for non-zero but small σ persists up to the SOC line $\sigma = 0$. If this scenario continues all the way to $\sigma = 0$, one must observe that the avalanche statistics there obey eq. (9) with the modified exponents. In fig. 4 we have verified this both for $d = 1, 2$. The data collapse according to eq. (9) for $P(s)$ and $P(T)$ are shown in fig. 4(a) and its inset, respectively. Figure 4(c) shows plots of $\langle s\rangle$ and $\langle T\rangle$ which clearly agree with the modified DP exponents $\tilde{\gamma} = 1$ and $\tilde{\tau} = \tau/\gamma$. This particular modification does not affect the DP scaling form $\langle s\rangle \sim \langle T\rangle^{\gamma/\tau}$. Indeed, the plot of $\langle s\rangle$ *vs.* $\langle T\rangle$ in the inset of fig. 4(c) shows that the DP exponent γ/τ is retained even in the SOC. The same scenario also holds in higher dimensions —figs. 4(b) and (d) demonstrate it for the driven dissipative Manna sandpile model in $2d$.

These results encourage us to propose that the critical behaviour of bulk dissipative SOC is only DP with rescaled exponents. To provide additional evidence next we study the stochastic sandpile models with discrete variables [6] by adding finite drive and diffusion.

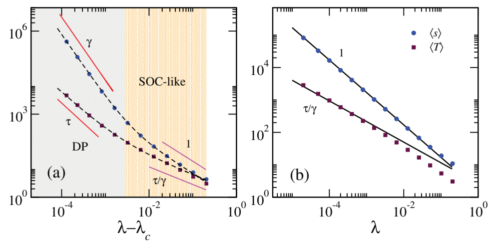

Fig. 5: (Colour on-line) Discrete Manna model ($1d$) with drive and dissipation: (a) the crossover from DP to SOC-like scaling for $\langle s\rangle$ and $\langle T\rangle$ against $\Delta = \lambda - \lambda_c$. Here $\sigma = 0.01$ and correspondingly $\lambda_c = 0.00757(1)$. The dashed lines are the best-fit curves following eq. (10). (b) Plot of $\langle s\rangle$ and $\langle T\rangle$ for $\sigma = 0$. The solid lines correspond to the modified exponents $\tilde{\gamma} = 1, \tilde{\tau} = 0.636$. Here $L = 10^4$ and the data are averaged over 10^5 or more ensembles.

Driven dissipative discrete Manna model. – The drive-dissipation mechanism can be extended to sandpile models with discrete variables. In the context of the Manna model, we consider a d-dimensional cube with each site $\mathbf{R}$ holding a *discrete* variable $n_{\mathbf{R}}$ called particle number —sites with $n_{\mathbf{R}} \geq n_c$, a predefined threshold (usually 2), hop independently to a randomly chosen neighbouring site $\mathbf{R}'$. Drive and dissipation can be implemented as follows.

I. *Dissipation*: All the sites belonging to $S_a \cup S_n$ attempt *independently* with probability λ to get vacated, *i.e.* to throw out all the particles out of the system,

$$n_{\mathbf{R}} \to 0 \quad \text{with probability } \lambda. \tag{11}$$

II. *Distribution*: The active sites which did not dissipate distribute their particles to the neighbouring sites; each particle independently moves to one of the neighbours.

III. *Drive*: Finally, the sites belonging to S_n, *i.e.* all the neighbours of active sites, are activated with probability σ, by receiving n_c particles

$$n_{\mathbf{R}} \to n_{\mathbf{R}} + n_c \quad \text{with probability } \sigma. \tag{12}$$

Unlike the continuous case (eqs. (2)–(4)) here λ denotes the probability with which a site decides to dissipate.

In the absence of drive and dissipation $\lambda = 0 = \sigma$ this dynamics only allows distribution of the particles of the active site and indeed is identical to the well-known fixed energy Manna model [6]. When the conserved particle density $\rho = \frac{1}{L}\sum_i n_i$ is tuned beyond the critical value $\rho_c = 0.89236$, this model undergoes an ordinary APT belonging to the directed percolation universality class [16]. On the other hand, in the maximal dissipation limit $\lambda = 1$ the dynamics once again becomes exactly that of site-directed percolation with active sites infecting their neighbours with probability σ. As expected, this shows an absorbing phase transition at $\sigma_c^{DP} = 0.705489$ [21]. For any non-zero $\sigma < \sigma_c^{DP}$, the discrete model undergoes a phase transition at a critical $\lambda_c < 1$, belonging to DP class (details are omitted here as this study closely follows the one for the continuous version).

Table 2: Connecting bulk and boundary dissipative SOC.

Dissipation:	Bulk	Boundary
Critical limit	$\lambda \to 0$	$L \to \infty$
$P(s)$	$\sim s^{-\tau_s} f(s\Delta^{\tilde{\kappa}_s})$ $\Rightarrow \langle s\rangle \sim \lambda^{-\tilde{\gamma}}$ $\tilde{\gamma} = \kappa_s(2-\tau_s)$	$\sim s^{-\tau_s} f\left(s/L^{D_s}\right)$ $\Rightarrow \langle s\rangle \sim L^{\mu_s}$ $\mu_s = D_s(2-\tau_s)$
$P(T)$	$\sim T^{-\tau_t} g(s\Delta^{\tilde{\kappa}_t})$ $\Rightarrow \langle T\rangle \sim \Delta^{-\tilde{\tau}}$ $\tilde{\tau} = \kappa_t(2-\tau_t)$	$\sim T^{-\tau_t} g\left(s/L^{D_t}\right)$ $\Rightarrow \langle T\rangle \sim L^{\mu_t}$ $\mu_t = D_t(2-\tau_t)$
Constraint	$\langle s\rangle \sim \lambda^{-1}$	$\langle s\rangle \sim L^2$

In the small drive-dissipation limit, $\langle s\rangle$ and $\langle T\rangle$ of the discrete model too show a crossover from DP to SOC-like scaling, which is described in fig. 5(a). The dashed lines here are the best fit to the data points according to eq. (10). Again for $\sigma = 0$, as shown in fig. 5(b), the ordinary DP feature is completely lost and one observes only SOC-like scaling. Thus, we conclude that the discrete version of the driven dissipative Manna model in $1d$ also shows a crossover from DP to SOC-like scaling, which continues all the way to the SOC line $\sigma = 0$.

Stochastic sandpile models with boundary dissipation. – Conventionally self-organised criticality is modeled with boundary dissipation and no additional drive (*i.e.* $\sigma = 0 = \lambda$). Usually a particle or unit energy is added to a randomly chosen site to initiate an avalanche which propagates following a conserving dynamics; avalanches which reach the boundary can dissipate particles at the boundary. With increasing system size, the dissipation rate decreases and accordingly the avalanche size increases such that, on the average, one particle is dissipated per cluster. Since the conserving bulk dynamics can be described by a diffusive process, the average size of avalanche $\langle s\rangle$ is proportional to the residence time of a random walker (starting from a random site) on the lattice with absorbing boundary,

$$\langle s\rangle \sim L^2, \tag{13}$$

where L is the linear size of the lattice. The similarity between (13) and $\langle s\rangle \sim \lambda^{-1}$ obtained for bulk dissipative models (in eq. (7)) is that both are derived from the requirement of stationarity and hold independently of the type or of the spatial dimension of the lattice.

It was shown in ref. [28] that cluster statistics of bulk dissipative SOC can be made equivalent to those obtained from boundary dissipation by using a system-size–dependent dissipation parameter λ. Following this argument, we use an equivalence $\lambda \sim L^{-2}$ to calculate the exponents of SOC models with boundary dissipation (see table 2) from the exponents obtained in this work. They can be expressed in terms of DP exponents as

$$\mu_t = 2\tilde{\tau} = \frac{2}{\gamma}\tau \quad \text{and} \quad D_{s,t} = 2\tilde{\kappa}_{s,t} = \frac{2}{\gamma}\kappa_{s,t}. \tag{14}$$

Table 3: The exponents obtained (from ref. [29]) for SOC models with boundary dissipation are compared with what one expects from the modified DP picture, *i.e.* from eq. (14).

	D_s	τ_s	D_t	τ_t
SOC($1d$)	2.253(14)	1.112(6)	1.445(10)	1.18(2)
eq. (13)	2.242	1.108	1.514	1.159
SOC($2d$)	2.750(6)	1.273(2)	1.532(8)	1.4896
eq. (13)	2.728	1.267	1.624	1.457

Note that $\tau_{s,t}$ are not affected, they remain the same as in ordinary DP. In table 3 we compare the recent numerical estimates of the exponents, measured in the discrete Manna model with boundary dissipation, with eq. (14). They are in good agreement —small discrepancies could come from discreteness (energy *vs.* particle). The study of continuous models, with boundary dissipation, is desirable.

Conclusion. – To summarize, in this paper we study absorbing phase transitions in stochastic sandpile models in the presence of bulk drive and dissipation, both coupled to activity. To facilitate the study of connection between SOC and DP, the stochastic sandpile model is designed in a way that in any dimension the dynamics reduces to site-directed percolation and self-organised criticality in two limiting cases. In addition to the generic DP critical behaviour, in the slow drive-dissipation regime the system shows a crossover in the subcritical phase from ordinary DP to SOC-like scaling. We explain that the exponents that characterise the emergent scaling regime are different, but can be expressed in terms of DP exponents. Moreover, this SOC-like scaling continues up to the zero dissipation line (SOC limit). Hence we argue that the critical behaviour of bulk dissipative SOC is only DP, modified by the dissipation control. We illustrate these phenomena explicitly for the continuous Manna model in $1d$ and $2d$, and its discrete version in $1d$. These results are not restrictive to the specific way we introduce drive and dissipation here. What is important is that they must be coupled to the activity field so that the absorbing configurations are not destroyed [30]. The specific drive-dissipation mechanism used here has an advantage —it maps to the site DP model for $\lambda = 1$.

Self-organized criticality in stochastic sandpile models, conventionally studied with boundary dissipation, is believed to belong to the Manna universality class. Our results in the context of bulk dissipative SOC suggest that what is ordinarily known as Manna class is possibly DP with modified exponents. It would be interesting to explore models with boundary dissipation from this point of view.

* * *

PKM would like to acknowledge the support of CEFIPRA under Project 4604-3.

REFERENCES

[1] Bak P., Tang C. and Wiesenfeld K., *Phys. Rev. Lett.*, **59** (1987) 381; *Phys. Rev. A*, **38** (1988) 364; Tang C. and Bak P., *Phys. Rev. Lett.*, **60** (1988) 2347.
[2] Dhar D. and Ramaswamy R., *Phys. Rev. Lett.*, **63** (1989) 1659.
[3] Zhang Y. C., *Phys. Rev. Lett.*, **63** (1989) 470.
[4] Dhar D., *Phys. Rev. Lett.*, **64** (1990) 1613.
[5] Grassberger P. and Manna S., *J. Phys. (Paris)*, **51** (1990) 1077.
[6] Manna S., *J. Phys. A: Math. Gen.*, **24** (1991) L363.
[7] Pietronero L., Tartaglia P. and Zhang Y. C., *Physica A*, **173** (1991) 22.
[8] Christensen K., Corral Á., Frette V., Feder J. and Jossang T., *Phys. Rev. Lett.*, **77** (1996) 107.
[9] Bak P., *How Nature Works: The Science of Self Organized Criticality* (Springer, Berlin) 1996; Dhar D., *Physica A*, **369** (2006) 29.
[10] Prussner G., *Self-Organised Criticality: Theory, Models and Characterisation* (Cambridge University Press) 2012.
[11] Vespignani A., Dickman R., Munoz M. A. and Zapperi S., *Phys. Rev. Lett.*, **81** (1998) 5676; Dickman R., Munoz M. A., Vespignani A. and Zapperi S., *Braz. J. Phys.*, **30** (2000) 27.
[12] Karmakar R. and Manna S. S., *Phys. Rev. E*, **69** (2004) 067107; Casartelli M., Dall'Asta L., Vezzani A. and Vivo P., *Eur. Phys. J. B*, **52** (2006) 91.
[13] Tadić B. and Dhar D., *Phys. Rev. Lett.*, **79** (1997) 1519.
[14] Mohanty P. K. and Dhar D., *Phys. Rev. Lett.*, **89** (2002) 104303; *Physica A*, **384** (2007) 34.
[15] Bonachela J. A. and Muñoz M. A., *Physica A*, **384** (2007) 89; *AIP Conf. Proc.*, **1091** (2009) 204.
[16] Basu M. *et al.*, *Phys. Rev. Lett.*, **109** (2012) 015702.
[17] Lee S. B., *Phys. Rev. E*, **89** (2014) 062133; da Cunha S. D., da Silva L. R., Viswanathan G. M. and Dickman R., arXiv:1405.1134.
[18] Lin C. Y. *et al.*, *Phys. Rev. E*, **74** (2006) 031304.
[19] Hwa T. and Kardar M., *Phys. Rev. Lett.*, **62** (1989) 1813.
[20] Paczuski M. and Bassler K. E., *Phys. Rev. E*, **62** (2000) 5347.
[21] Henkel M., Hinrichsen H. and Lübeck S., *Non-Equilibrium Phase Transitions*, Vol. **1** (Springer, Berlin) 2008; Hinrichsen H., *Adv. Phys.*, **49** (2000) 815.
[22] Janssen H. K., *Z. Phys. B*, **42** (1981) 151; Grassberger P., *Z. Phys. B*, **47** (1982) 365.
[23] Supplementary text: `www.saha.ac.in/cmp/pk.mohanty/SOC.pdf`.
[24] Muñoz M. A., Dickman R., Vespignani A. and Zapperi S., *Phys. Rev. E*, **59** (1999) 6175.
[25] On the contrary, an active seed is created in FES by *transferring* energy from other sites, so that conservation is maintained.
[26] The energy balance condition for stationarity $1 + b\sigma\langle s\rangle = a\lambda\langle s\rangle$, with constants a and b leads to $\langle s\rangle \sim (\lambda - b\sigma/a)^{-1}$. On the l.h.s., 1 corresponds to the initially added energy.
[27] Shilo Y. and Biham O., *Phys. Rev. E*, **67** (2003) 066102.
[28] Malcai O., Shilo Y. and Biham O., *Phys. Rev. E*, **73** (2006) 056125.
[29] Huynh H. N. and Pruessner G., *Phys. Rev. E*, **85** (2012) 061133.
[30] Basu U., Basu M. and Mohanty P. K., *Eur. Phys. J. B*, **86** (2013) 236.